Application of hyperspectral imaging to discriminate waxy corn seed vigour after aging

[1]Yuan, P., [2]Pang, L., [1]Wang, L. M. and [1]*Yan, L.

[1]School of Technology, Beijing Forestry University, Beijing, 100083, China
[2]Institute of Artificial Intelligence in Sports, Capital University of Physical Education and Sports, Beijing, 100191, China

Abstract

A hyperspectral imaging system covering 400 - 1000 nm spectral range was applied for vigour detection of waxy maize seeds after artificial aging. After spectral pre-processing, the characteristic wavelength was selected by uninformative variable elimination (UVE), competitive adaptive reweighted sampling (CARS), and random frog (RF) methods. The moisture, starch, protein, and fat contents were measured for each grade of seed, and these values were correlated with the spectrum. Finally, the vitality detection model was established by least squares support vector machine (LS-SVM), extreme learning machine (ELM), and random forest (RF). The prediction sets exhibited high classification accuracy (> 99%) for 115 features. The model constructed from the bands significantly correlated with chemical composition (CC), and was better than the classic feature selection methods. The overall results indicated that hyperspectral imaging could be a potential technique to assess seed vigour.

Introduction

Waxy corn (*Zea mays* L. *sinensis Kulesh*) originated in China as a mutation of hard corn. This crop has high economic, nutritional, and processing values, and has become very popular in the corn industry. Waxy corn kernels have higher nutrient content than that in common corn, with 70 - 75% starch, more than 10% protein, and 4 - 5% fat. During storage, seeds undergo physiological and physiochemical changes including deterioration of seed chemistry (Kapoor *et al*., 2011; Eisvand *et al*., 2016). This natural aging is a long-term process, and aging study requires extensive sampling. As an alternative, artificially accelerated aging can be performed in the laboratory to simulate seed aging to facilitate and expedite the study (Men *et al*., 2017).

Like in traditional corn, the seed vigour of waxy corn is directly related to its seed germination performance and emergence. Conventional methods used to estimate seed viability include germination, tetrazolium (TZ), and electric conductivity tests (Kandpal *et al*., 2016). However, these traditional methods are time-consuming, laborious, and seed-damaging. Fourier near infrared (Altameme *et al*.,

2015; Qiu *et al*., 2019), near-infrared (Rodríguez-Pulido *et al*., 2014; Jia *et al*., 2015), and Raman spectroscopy methods (Lee *et al*., 2017) are newer methods that can be applied to the study of seeds. However, these approaches typically do not obtain sufficient information by using point-based scanning techniques.

Hyperspectral imaging technology is a new non-destructive testing method that combines imaging and spectral data (Xia *et al*., 2019). In recent years, this approach for seed quality evaluation has received extensive attention and application in various fields, especially agricultural and forestry. This technique has been applied to seed type differentiation (Wang *et al*., 2016; Zhao *et al*., 2018), internal main component detection (Yang *et al*., 2018), origin (Gao *et al*., 2013), storage time assessment (Guo *et al*., 2017), seed infection detection (Kimuli *et al*., 2018; Polder *et al*., 2019), and seed vigour prediction (Ambrose *et al*., 2016; Wakholi *et al*., 2018). Zhang *et al*. (2018) compared partial least squares discriminant analysis (PLS-DA) and support vector machines (SVM) models, finding that the PLS-DA model had high classification accuracy for whole wheat seeds (> 85.2%) and viable

seeds (> 89.5%) by using only 16 wavebands. Snider *et al*. (2016) studied the effects of cotton seed chemical composition on seedling vigour, concluding that seed quality and also oil and protein content positively correlated with seedling vigour. Cai *et al*. (2013) found a positive correlation of soluble protein with seed vigour. These applications of hyperspectral imaging technology successfully predicted components and vitality of different seeds, but further work is required to correlate spectral values and main components for vitality assessment.

For the identification of waxy corn seed vigour using hyperspectral imaging, the goal of the present work was to perform component-related feature band selection to improve the model discriminative ability. The specific steps of this approach were: (1) to obtain the hyperspectral information of different varieties of glutinous maize seeds subjected to different lengths of aging duration, and then measure seed vigour by standard germination experiments; (2) to analyse the correlation of main chemical components and spectra in seeds; (3) to perform spectral pre-processing and select characteristic bands to establish a classification model; and (4) to assess the ability to predict the level of vigour of different varieties of waxy corn seeds.

Materials and methods

Sample preparation

Two breeds of waxy corn seeds, Jingkenuo 2000 and Zhongpintiannuo F1, were purchased from the Beijing Seed Company, Beijing, China. For each breed of waxy corn, 1,400 g (about 4,000 grains) were divided into four groups, and subjected to different aging durations. The control group was not aged, but kept at room temperature. The other three groups were placed in an artificial aging tank at 45°C (Qiu *et al*., 2019) and relative humidity of 98% for 3, 6, or 9 d. The four grades for both Jingkenuo 2000 and Zhongpintiannuo F1 breeds resulted in eight categories, designated as A, B, C, D, E, F, G, and H. The 288 samples in each group were used for data analysis, for a total of 2,304 samples.

Measurements of seed chemical components

To provide sufficient sample size for the experiment, 300 g seeds were arbitrarily chosen from each category, and the water, protein, starch, and fat contents were measured. To this end, 75 g samples were divided into three groups for three separate measurements, and then, these three measurements were averaged. The above components were measured in accordance with the National Food Safety Standard of the People's Republic of China using direct drying, acid hydrolysis, Kjeldahl, and Soxhlet extraction methods (Chinese Standard, 2016a; 2016b; 2016c; 2016d). All test results are presented in Table 1.

Table 1. Major components (g/100 g) of eight groups of waxy corn seeds.

Component	A	B	C	D	E	F	G	H
Moisture	9.06	8.29	7.93	7.81	9.7	8.68	8.1	7.77
Starch	44.3	26.3	45.6	29.2	65.6	36	34.7	43.3
Protein	10.8	9.7	9.5	9	11.1	10.3	10.6	10
Fat	4.1	3.7	4.5	3.6	4.2	4.3	4.6	4.5

Hyperspectral image acquisition and correction

The hyperspectral image system included an SOC710 imaging spectrometer with a built-in C-type infrared correction lens (Surface Optics Corporation, USA), two 250 W halogen lamps (OSRAM GCA, Guangdong, China), tilted to 45° and placed symmetrically, a transport platform, and a computer terminal. This instrument has a spectral range of 400 - 1000 nm, a spectral resolution of 4.6875 nm (115 bands in total), and collects an image of 520 × 696 pixels.

For imaging, 288 samples were randomly selected from the remaining 200 g samples of each

treatment class, and hyperspectral data were collected. The waxy corn seeds were set in a Petri dish (9 cm Ø), with 22 cm distance between the container and imaging spectrometer. After collecting hyperspectral images, the original images (I_R) were calibrated to remove noise. The black reference (I_B) was acquired when the camera lens was covered, and the white reference (I_W) was collected using a white Teflon board with approximately 100% reflectance. The corrected image (I) was calculated using Eq. 1:

$$I = \frac{I_R - I_B}{I_W - I_B}$$ (Eq. 1)

Standard germination test

Waxy corn seeds with hyperspectral information were subjected to standard germination test. Samples were placed in a separate Petri dishes with filter paper that was soaked with water to retain moisture. Following 7-d incubation at 25°C with 99% relative humidity and continuous light in the incubator, the germination was measured. According to the International Seed Testing Association standard (ISTA, 2015), if the germ of the seed is larger than 1 cm, it is considered a viable seed. The germination rates of the eight categories were 83.3, 95.8, 91.7, 54.2, 89.6, 93.8, 75.0, and 47.9% (corresponding to groups named A, B, C, D, E, F, G, and H), respectively. Short-term high temperature treatment can promote the improvement of seed vigour, consistent with Yan *et al*. (2014) study of oak (*Quercus liaotungensis*) seeds. The germination rate and average root length both initially increased and then decreased with the increase of aging duration.

Spectral extraction and pre-processing

The selection of an appropriate region of interest (ROI) is critical because it affects the extraction of the spectral data. Adaptive threshold segmentation is widely used due to its simplicity and efficiency, and was used for ROI selection in the present work (Karasulu and Korukoglu, 2010). Spectral extraction was done in four steps. The reflected image at 743.79 nm was chosen as this yielded the highest contrast between the seed and background (step I). Next, the binary image was established based on the grayscale image, and then, filtering was performed to enhance the binary image and eliminate noise (step II). The complete single area of each seed was set as the ROI (step III). Finally, the average spectrum of seeds was calculated from the average of the intensity values of all pixels in the ROI for each seed in 115 bands (step IV).

Multiplicative scatter correction (MSC) can effectively eliminate the effect of scattering, and enhance the spectral absorption information related to different components. Savitzky-Golay (SG) first derivative pre-processing is used to separate small absorption peaks, and improve spectral resolution. In the present work, MSC and SG first derivative methods were combined to remove the noise from the spectrum data and improve the prediction ability.

Optimal wavelength selection

Hyperspectral data are typically large, but contain a lot of redundant information, thus requiring extensive computing time and storage space for data processing. Uninformative variable elimination (UVE) (Cai *et al*., 2008), a commonly used method for variable selection, aims to select the best combination of important variables while removing useless information to improve verification performance. This method uses the partial least squares (PLS) regression coefficient as an indicator of wavelength importance.

Competitive adaptive reweighted sampling (CARS) (Li *et al*., 2009) is a variable selection method based on the principle of 'survival of the fittest' in Darwinian evolution theory. This method combines the exponentially decreasing function (EDF) and adaptive reweighted sampling technique (ARS) to select the variable point with the larger absolute value of the regression coefficient in the PLS model, and remove the variable point with the smaller weight value (Wang *et al*., 2017). Cross-validation can then be used to select the smallest root mean square error calculated from the cross-validation (RMSECV) subset in the PLS subset model. The variables contained in this subset are the optimal combination of variables.

Random frog (RF) (Bao *et al*., 2019) calculates the probability of being selected for each variable by simulating a Markov chain based on a steady state distribution. Whether the variable is selected or eliminated during each iteration is based on the size of the absolute value of each variable on the regression coefficient curve in the returned results.

Recognition model development

The least squares support vector machine (LS-SVM) starts from the loss function of machine learning, and uses the second norm in the objective function of the optimisation problem. Additionally, the inequality constraints in standard support vector machine (SVM) algorithms are replaced by equality constraints. In this way, the LS-SVM method changes the optimisation problem to a set of linear equations, which increases calculation efficiency over that of SVM, and improves the accuracy and precision of processing non-linear signals (Su *et al*., 2015). Radial basis function (RBF) was chosen as the kernel function of LS-SVM.

Extreme learning machine (ELM) is a type of machine learning system or method based on a feedforward neural network. In this kind of system,

the weights of hidden layer nodes are given randomly or artificially, no updating is needed, and the learning process only calculates output weights (Huang *et al*., 2006). For single hidden layer neural networks, ELM can randomly initialise input weights and biases to get the corresponding output weights. The connection weights between the hidden layer and the output layer do not need to be adjusted iteratively, but instead are determined a single time by solving the system of equations. ELM is widely used in computer vision, bioinformatics, and in regression problems in some earth and environmental sciences (Huang *et al*., 2015).

By integrating multiple trees through ensemble learning, a random forest (RF) is formed with a decision tree as the basic unit. The construction method of each decision tree is as follows: (1) N represents the number of samples, and M represents the number of features; (2) the input m (m is far less than M) is used to determine the result of the previous node of the decision tree; (3) for a sample with replacement in N samples, repeating N times is performed to form a training set, and prediction with unsampled ones; and (4) for each node, m features are randomly selected to calculate the best splitting method. In this way, a complete tree is constructed. RF can effectively run-on large data sets, process input samples with high-dimensional features, and obtain good results for the default value problem (Breiman, 2001).

Results and discussion

Spectral features

Figure 1 shows the similarity of the average spectra and the difference in reflectance for all tested grades of seeds. All spectra were pre-processed by MSC and SG first derivative methods. This treatment removed scattering effects, and made it easier to distinguish multiple peaks and valleys. Crests and troughs of the short-wave near-infrared region are often caused by stretching and frequency doubling of the bending vibration of the X-H (N-H, C-H, O-H) bonds of proteins (Schrieve *et al*., 1991). It can be seen from the figure that after the same aging treatment, the average spectra of the seeds of Jingkenuo 2000 and Zhongpintiannuo F1 had obvious aggregation. Among them, the control group was particularly obvious, which was well distinguished from other grades. The vitality curves for all samples after pre-processing exhibited similar trends over the

entire band, with some overlap in spectra. Therefore, chemometric methods were necessary for further classification and identification.
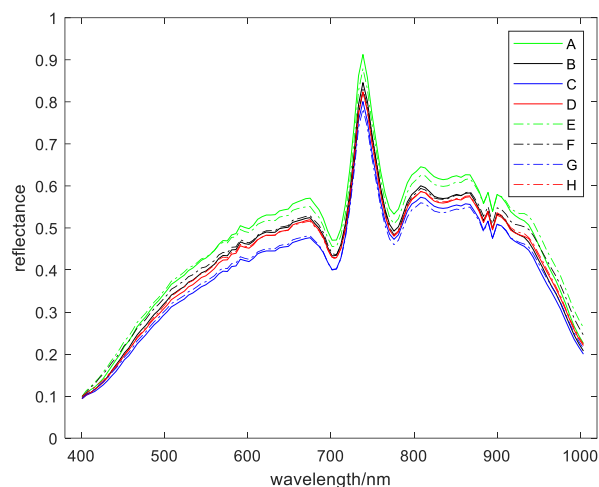

Figure 1. Average spectra of eight groups of waxy corn seeds.

Reference analysis of chemical composition

The main components of seeds will be affected by genetic factors, as well as by external environmental factors such as climate and soil conditions, harvest time, maturity, processing, packaging, transportation, and storage. The main components of seeds subjected to different storage conditions may be the same, but there may be variation in content, thus resulting in changes in the spectrum. The hyperspectral study of seed vigour requires good correlations between the spectrum and the main components of seeds.

The water, starch, protein, and fat contents varied in different types of waxy corn with different aging durations. Table 2 shows the contents of each major storage substance per 100 g of sample. With increased aging duration, the moisture content of seeds in the same category showed a decreasing trend. The amount of the primary substance in corn seeds, starch, also decreased suddenly with aging. Only small changes in protein and fat contents were observed, with the same decreasing trend. This may reflect changes in different enzyme activities during aging (Zhu *et al*., 2018; Wang and Ju, 2019). Enzymes and other substances could together increase the total amounts of starch, protein, and lipids in seeds.

A primary goal of the present work was to correlate the amounts of different components and the spectral data (average spectrum) of the eight groups

of seeds. The Pearson correlation coefficient method was used, and the correlation coefficient (R) and the test *p* value were determined. R was used to assess the correlation between the spectrum and the composition of a component, and the *p* value was used to assess significance. Characteristic bands of R > 0.8 and *p* < 0.05 were selected for the four

components of each category of the two categories of seeds, as shown in Table 2. The repeated parts of these bands were removed for subsequent modelling, as is done in conventional feature selection methods. Therefore, a total of 44 bands were extracted as feature bands.

Table 2. Extraction of bands significantly related to the main storage components.

Variety	Component	Number of bands	Wavelength (nm)
Jingkenuo 2000	Moisture	3	632.8, 727.8, 786.5
	Starch	7	765.1, 770.5, 775.8, 797.2, 802.6, 845.6, 965.2
	Protein	4	400.6, 727.8, 786.5
	Fat	8	482.3, 518.3, 717.2, 722.5, 754.5, 759.8, 840.2, 851.0
Zhongpintiannuo F1	Moisture	10	400.6, 441.3, 446.4, 461.8, 528.7, 781.2, 905.2, 970.7, 976.2
	Starch	8	523.5, 669.6, 674.9, 680.2, 749.1, 872.6, 878.1, 954.3
	Protein	2	533.8, 910.6
	Fat	13	431.1, 446.4, 451.5, 461.8, 690.7, 754.5, 781.2, 802.6, 851.0, 867.2, 926.9, 932.4, 937.9

Feature band extraction by different methods

A total of 115 features were included in the modelling based on the raw data, but there may be some redundant information in these features. To select valid information and improve operation speed, UVE, CARS, and RF methods were used to extract the characteristic bands from the original bands. When using the UVE method for selection, the optimal number of major factors was set to eight. The best results were obtained when the upper and lower thresholds were +68 and -68, respectively, and the minimum RMSECV reached the minimum value of 0.1770. This gave 43 characteristic bands. The CARS algorithm reduced the number of variables from 115 to 50. Five cross-validations were performed with 300 Monte Carlo samples. When RF was applied, the maximum number of latent variables for cross-validation when using the automatic scaling method was eight, and 32 characteristic bands were finally selected.

The bands significantly correlated with the chemical composition (CC) based on these three methods were compared. Figure 2 shows the number

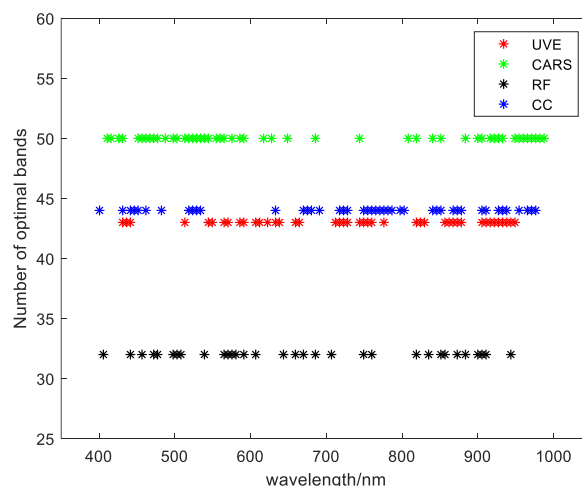of characteristic bands selected by each method, and the specific location of each band.

Figure 2. Comparison of feature bands selected by different feature selection methods.

The bands selected by CARS had obvious two-end differentiation, with more features in the 400 - 600 and 800 - 1000 nm ranges, but sparse signal in

the 600 - 800 nm range. UVE and RF patterns were relatively uniformly distributed over the entire band. In the 500 - 700 nm range, CC had an interval close to 100 nm, and its characteristic band was more concentrated in the near-infrared spectral range.

Discriminant model based on different feature sets

To compare the different classification methods to detect and classify the corn seed spectral data and increase reliability, LS-SVM, ELM, and RF methods were employed to establish discriminant models for different grade of waxy corn seeds. For modelling, 288 seeds in each of eight groups were divided into three equal portions, and then randomly build a single calibration set and prediction set at a ratio of 2:1. Combining them, the sample sizes of the prediction set and calibration set were 768 and 1,536, respectively, during each modelling. This was done

three times, and the average was considered the final classification result.

Table 3 summarises the results of discriminant models under different models and different feature sets. With 115 features in the full band, both the LS-SVM and RF calibration sets could achieve 100% accuracy, with higher prediction set accuracy for the LS-SVM model (about two percentage points). All three modelling methods gave similar results with fewer features, though was done as good as the full-band result. When compared with the results of the full-band prediction set, the feature model results were 0.69 - 7.59% less accurate. This result differs from that of Kandpal *et al*. (2016) who used PLS-DA to establish a melon seed vigour model, and found that the model with characteristic band selection by VIP and SR was similar to or better than the full band model.

Table 3. Recognition results of different discriminant models based on different sets of bands.

Discriminant model		Number of characteristic band (%)				
		115 (Full[1])	43 (UVE)	50 (CARS)	32 (RF)	44 (CC[2])
LS-SVM	Cal.[3]	100	100	100	100	100
	Pre.[4]	99.22	96.88	97.74	98.18	98.53
ELM	Cal.	91.71	89.94	90.8	84.81	89.91
	Pre.	86.93	86.11	86.46	79.34	86.72
RF	Cal.	100	100	100	100	100
	Pre.	97.31	93.31	94.36	90.8	96.61

[1]full band characteristics, [2]bands correlated with the main chemical composition, [3]calibration set, and [4]prediction set.

UVE, CARS, and RF are classic and reliable feature selection methods. In the SVM model of wheat variety classification, RF feature selection allowed the use of 50 bands for results that were similar to those obtained using 256 bands (Bao *et al*., 2019). These methods all performed well in the present work. For the LS-SVM model, the accuracy of the training set was 100%, and the accuracy of the prediction set remained stable at greater than 96%. Modelling with ELM and RF was less successful, with poor performance based on RF characteristic bands. This may be due to the small number of bands, and the relatively discrete distribution. CC may be the optimal feature selection method, with recognition capabilities superior to the other three feature selection methods. The first three classic methods only used spectral data to select the most representative band. The CC method required only 44

bands to achieve close to the full-band effect. These 44 bands were significantly related to the main storage substances in waxy corn seeds, and could fully reflect the role of chemical components on the spectrum. The results obtained in the present work will facilitate the development and use of spectral methods to study seed composition and vigour.

Conclusion

Hyperspectral imaging technology allowed for the successful determination of the vigour of waxy maize seeds subjected to different aging times. Correlation analysis was performed between the spectral data and the levels of water, protein, starch, and fat; and 44 bands with significant correlation were identified. UVE, CARS and RF were also used for feature selection. Among the discriminant models

established by LS-SVM, ELM, and RF, the LS-SVM was the best, with good stability under different characteristic bands. In these models, the accuracy recognition rate of eight grades of seeds was over 96%. For feature selection, the CC selected band was more conducive for model establishment. The spectrum exhibited a strong correlation with the main chemical substances in seeds. The results of the present work showed that hyperspectral technology could effectively detect seed vigour for waxy corn seeds of different species and vigour. In future studies, waxy maize seeds of different varieties and vigour levels should be tested. More substances related to seed vigour should be measured, and the correlation analysis of substances related to vigour should be carried out to establish the basis for use of hyperspectral imaging technology to detect seed vigour.

Acknowledgement

References

Altameme, H., Hameed, I. H. and Abu-Serag, H. A. 2015. Analysis of bioactive phytochemical compounds of two medicinal plants, *Equisetum arvense* and *Alchemila valgaris* seeds using gas chromatography-mass spectrometry and Fourier-transform infrared spectroscopy. Malaysian Applied Biology 44(4): 47-58.

Ambrose, A., Kandpal, M. L., Kim, M. S., Lee, W. H. and Cho, B. K. 2016. High speed measurement of corn seed viability using hyperspectral imaging. Infrared Physics and Technology 75: 173-179.

Bao, Y. D., Mi, C. X., Wu, M., Liu, F. and He, Y. 2019. Rapid classification of wheat grain varieties using hyperspectral imaging and chemometrics. Applied Sciences 9: article no. 4119.

Breiman, L. 2001. Random forests. Machine Learning 45(1): 5-32.

Cai, C. J., Fan, S. H., Liu, H. and Cao, B. H. 2013. Physiological and biochemical changes of moso bamboo (*Phyllostachys edulis*) seeds in artificial aging. Scientia Silvae Sinicae 49(8): 29-34.

Cai, W. S., Li, Y. K. and Shao, X. G. 2008. A variable selection method based on uninformative variable elimination for multivariate calibration of near-infrared spectra. Chemometrics and Intelligent Laboratory Systems 90(2): 188-194.

Chinese Standard. 2016a. GB 5009.3-2016 - determination of moisture in food. People's Republic of China: National Standard of the People's Republic of China.

Chinese Standard. 2016b. GB 5009.5-2016 - determination of protein in food. People's Republic of China: National Standard of the People's Republic of China.

Chinese Standard. 2016c. GB 5009.6-2016 - determination of fat in food. People's Republic of China: National Standard of the People's Republic of China.

Chinese Standard. 2016d. GB 5009.9-2016 - determination of starch in food. People's Republic of China: National Standard of the People's Republic of China.

Eisvand, H., Moori, S., Ismaili, A. and Sasani, S. 2016. Effects of late-season drought stress on physiology of wheat seed deterioration: changes in antioxidant enzymes and compounds. Seed Science and Technology 44(2): 1-15.

Gao, J. F., Li, X., Zhu, F. L. and He, Y. 2013. Application of hyperspectral imaging technology to discriminate different geographical origins of *Jatropha curcas* L. seeds. Computers and Electronics in Agriculture 99: 186-193.

Guo, D. S., Zhu, Q. B., Huang, M., Guo, Y. and Qin, J. W. 2017. Model updating for the classification of different varieties of maize seeds from different years by hyperspectral imaging coupled with a pre-labeling method. Computers and Electronics in Agriculture 142: 1-8.

Huang, G. B., Zhu, Q. Y. and Siew, C. K. 2006. Extreme learning machine: theory and applications. Neurocomputing 70: 489-501.

Huang, G., Huang, G. B., Song, S. and You, K. 2015. Trends in extreme learning machines: a review. Neural Networks 61: 32-48.

International Seed Testing Association (ISTA). 2015. International rules for seed testing. United States: ISTA.

Jia, S. Q., An, D., Liu, Z., Gu, J. C., Li, S. M., Zhang, X. D., … and Yan, D. 2015. Variety identification method of coated maize seeds based on near-infrared spectroscopy and chemometrics. Journal of Cereal Science 63: 21-26.

Kandpal, L. M., Lohumi, S., Kim, M. S., Kang, J. S. and Cho, B. K. 2016. Near-infrared hyperspectral imaging system coupled with multivariate methods to predict viability and vigor in muskmelon seeds. Sensors and Actuators B - Chemical 229: 534-544.

Kapoor, N., Arya, A., Siddiqui, M. A., Kumar, H. and Amir, A. 2011. Physiological and biochemical changes during seed deterioration in aged seeds of rice (*Oryza sativa* L.). American Journal of Plant Physiology 6: 28-35.

Karasulu, B. and Korukoglu, S. 2010. A simulated annealing-based optimal threshold determining method in edge-based segmentation of grayscale images. Applied Soft Computer 11(2): 2246-2259.

Kimuli, D., Wang, W., Lawrence, K. C., Yoon, S. C., Ni, X. Z. and Heitschmidt, G. W. 2018. Utilisation of visible/near-infrared hyperspectral images to classify aflatoxin B_1 contaminated maize kernels. Biosystem Engineering 166: 150-160.

Lee, H., Kim, M. S., Qin, J. W., Park, E., Song, Y. R., Oh, C. S. and Cho, B.-K. 2017. Raman hyperspectral imaging for detection of watermelon seeds infected with *Acidovorax citrulli*. Sensors 17(10): article no. 2188.

Li, H. D., Liang, Y. Z., Xu, Q. S. and Cao, D. S. 2009. Key wavelengths screening using competitive adaptive reweighted sampling method for multivariate calibration. Analytica Chimica Acta 648: 77-84.

Men, S., Yan, L., Liu, J. X., Qian, H. and Luo, Q. J. 2017. A classification method for seed viability assessment with infrared thermography. Sensors 17: article no. 845.

Polder, G., Blok, P. M., Villiers, H. A., Wolf, J. M. and Kamp, J. 2019. Potato virus Y detection in seed potatoes using deep learning on hyperspectral images. Frontiers in Plant Science 10: 1-13.

Qiu, G. J., Lü, E., Wang, N., Lu, H. Z., Wan, F. and Zeng, F. G. 2019. Cultivar classification of single sweet corn seed using Fourier transform near-infrared spectroscopy combined with discriminant analysis. Applied Sciences 9(8): article no. 1530.

Rodríguez-Pulido, F. J., Hernández-Hierro, J. M., Nogales-Bueno, J., Gordillo, B., González-Miret, M. L. and Heredia, F. J. 2014. A novel method for evaluating flavanols in grape seeds by near infrared hyperspectral imaging. Talanta 122: 145-150.

Schrieve, G. D., Melish, G. G. and Ullman, A. H. 1991. The Herschel-infrared—a useful part of the spectrum. Applied Spectroscopy 145: 711-714.

Snider, J. L., Collins, G. D., Whitaker, J., Chapman, K. D. and Horn, P. 2016. The impact of seed size and chemical composition on seedling vigor, yield, and fiber quality of cotton in five production environments. Field Crops Research 193: 186-195.

Su, Z., Tang, B., Liu, Z. and Qin, Y. 2015. Multi-fault diagnosis for rotating machinery based on orthogonal supervised linear local tangent space alignment and least square support vector machine. Neurocomputing 157: 208-222.

Wakholi, C., Kandpal, L. M., Lee, H., Bae, H., Park, E., Kim, M. S., … and Cho, B.-K. 2018. Rapid assessment of corn seed viability using short wave infrared line-scan hyperspectral imaging and chemometrics. Sensors and Actuators B - Chemical 255: 498-507.

Wang, C. L. and Ju, F. C. 2019. Study on seed vigor and physiological characteristics of hybrid maize varieties during aging. Seed 38(10): 97-100.

Wang, H. L., Yang, G. G., Zhang, Y., Bao, Y. D. and He, Y. 2017. Detection of fungal disease on tomato leaves with competitive adaptive reweighted sampling and correlation analysis methods. Spectroscopy and Spectral Analysis 37(7): 2115-2119.

Wang, L., Sun, D. W., Pu, H. B. and Zhu, Z. W. 2016. Application of hyperspectral imaging to discriminate the variety of maize seeds. Food Analytical Methods 9: 225-234.

Xia, J. A., Cao, H. X., Yang, Y. W., Zhang, W. X., Wan, Q., Xu, L., … and Huang, B. 2019. Detection of waterlogging stress based on

hyperspectral images of oilseed rape leaves (*Brassica napus* L.). Computers and Electronics in Agriculture 159: 59-68.

Yan, X. F., Qiu, Z. H., Du, Q., Zhang, Q. and Qin, W. C. 2014. Influences of seed coat and temperature on the germination of *Quercus wutaishanica* seeds. Journal of Northwest Forestry University 29(3): 119-124.

Yang, G. Y., Wang, Q. Y., Liu, C., Wang, X. B., Fan, S. X. and Huang, W. Q. 2018. Rapid and visual detection of the main chemical compositions in maize seeds based on Raman hyperspectral imaging. Spectrochimica Acta Part A - Molecular and Biomolecular Spectroscopy 200: 186-194.

Zhang, T. T., Wei, W. S., Zhao, B., Wang, R. R., Li, M. L., Yang, L. M., … and Sun, Q. 2018. A reliable methodology for determining seed viability by using hyperspectral data from two sides of wheat seeds. Sensors 18(3): article no. 813.

Zhao, Y. Y., Zhu, S. S., Zhang, C., Feng, X. P., Feng, L. and He, Y. 2018. Application of hyperspectral imaging and chemometrics for variety classification of maize seeds. RSC Advances 8: 1337-1345.

Zhu, Y. Z., Xia, L. M., Zhu, S. Y., Liu, J., Yang, R., Wang, Q., … and Feng, F. 2018. Changes of vigor, physiological characteristics and genetic diversities of artificially aged sweet corn seeds. Journal of South China Agricultural University 39(1): 25-30.